Author response to the referees' comments

Dear referees and editor,

We are very grateful for your positive comments and constructive suggestions on our manuscript "*A Lagrangian-based Floating Macroalgal Growth and Drift Model (FMGDM v1.0): application in the green tides of the Yellow Sea*". Following these comments and suggestions, we have revised this manuscript. In particular, We 1) added additional validations for the Lagrangian tracking module through a comparison with the observed surface and subsurface drifters, 2) upgraded the macroalgal growth model with the inclusion of nutrient's influences, 3) made the adjustments of initial deployments of *U. prolifera* around its origin region, and 4) re-ran all cases and updated all results based on these re-configurations.

Our response to the comments of each referee and corresponding changes are provided in this document, with a **bold** front for comments and a regular front for our answers. The manuscript quotations are represented in *italics*, and the changes in the manuscript are highlighted as underlined. The introductory parts of the referee report are omitted and marked as […] to keep the document concise.

We hope that our response can address the referee's concerns sufficiently.

Sincerely,

Fucang Zhou and Jianzhong Ge (on behalf of the author team)

Referee comment #1

[…] Although some bias still existed, this is acceptable considering the complex influencing factors in the system. What is more remarkable is that this model can simulate the coverage and biomass of the floating macroalgae much better when using short-term modeling. This is pretty useful for predicting when green tides are happening.

Thanks. We have significantly improved the manuscript to address the reviewers' comments. For details, please see the responses to the other two reviewers below.

Referee comment #2 and #3

From comment #2, part 1:

[…] Yet it fails to capture the year to year variability seen in the satellite product – in magnitude and extent –, suggesting important drivers of U. prolifera are not represented. Overall, the structure of the paper could be improved, so does the writing as abbreviations and typos are presents. I do not think that the experimental set-up is sufficiently convincing to ascertain that these results are robust.

1. **the validation of the Lagrangian transport for supporting the choice of ocean model and fraction of the wind component for the windage is not robust; the authors set windage on 3.5% without having completed a sensitivity analysis or referencing a study that did so. Macroalgae are influenced by wind yet the fraction depends on the physical characteristics of the floating object. The passive drifting experiments should be carried out with a much larger number of particles in the order of tens of thousands (currently only 6), and released over a wider period (currently simply a single date instead of across a full month of prolifera observed presence in the release area). Density maps of particle positions after 120 days for each experiments (ocean currents only, and different windage factors) should be provided to illustrate the differences in drifting patterns, together with a thorough**

argumentation for the choice in the balance of ocean current and windage for U. prolifera drifting. I also suggest the use of the Global Drifting Program dataset (if sufficient floats are available in the area) to evaluate drifting patterns in the region using drogued vs undrogued surface floats (that remove or include a wind factor), and evaluate the model skills in reproducing the patterns from observations. Such work would also benefit the interpretation of the patterns obtained with the individual based growth model, in order to disentangle influence of biology and physics to explain biomass distribution.

From comment #3, part 1:

[…] However, the paper is missing some important details and background information. Here are some specifics:

1. **Windage is assumed to be 1.5% to 3.5%, but the authors do not explain why this value was taken. As the authors pointed out with the simulations without wind, wind plays a crucial role in determining trajectories. Please cite references and detail your reasoning behind this selection. The authors should determine if the surface layer of the hydrodynamic solution already represents some movement due to wind. The authors may consider looking at analagous studies with large floating objects (e.g., tsunami debris) or drifter studies to calibrate windage.**

Our responses to the uncaptured annual variability of green tide and our attempt to solve this problem are given in our replies to the referrer's comment #2, part 4. Here, we first respond to the comment about windage, which both referees raised. Then, following the referee's suggestions, we have conducted a series of experiments on windage range in 2.7-3.5% and added the experimental results in Section 3.2.2. Additionally, more supporting references were cited in the revision to select a more appropriate windage coefficient.

To reduce the computational load, we used the super-particle approach. A super-particle was defined as an ensemble particle accounting for 100 tons of *U. prolifera.* This approach is commonly used in larval transport studies. Examples can be seen in recent scallop larval transport studies done by (Chen et al., 2021). Considering the rapid algal growth during the bloom outbreak, the individual number of *U. prolifera* could increase up to >15000 at the peak of the bloom. In the revision, we have increased the initial number of particles to 480, 10 times more than the number used in our last submission. To better compare drifting patterns under different windage, we remain the initial particle release on May 1. In the realistic simulations of green tides, we released the particles continuously over an entire month, as the referees suggested.

Regarding the validation of particle tracking in the Yellow Sea and adjacent regions, we checked the Global Drifting Program dataset to search the data in the region. Unfortunately, the dataset does not cover our study areas. Luckily, we found some drifter trajectory data in our region from Bao et al. (2015). We used these data to evaluate the skills of our particle tracking algorithms and the accuracy of the hydrodynamic model ECS-FVCOM. In addition, we also conducted a drogued-drifter experiment in the nearby East China Sea area over the summer of 2017. The results of these additional studies were added in the revision to strengthen the model validation. See the detail below.

By the way, the hydrodynamic surface layer had already included a 1.5% wind effect, and the other wind drags for particles drifting were composed by direct windage.

The modification contained two parts in the revision: a) the windage experiments and b) the tracking model validation.

a) The revised windage experiments.

In section 2.7, the model configuration is revised.

For the wind-exposed drifters floated at the sea surface, the wind drift is one of dominating contributions of the transportation. Dagestad and Röhrs (2019) conducted drifting buoy experiments and found that windage accounted for 3% of Stokes drift. Whiting et al. (2020) chose a constant 3% coefficient in the free-floating macroalgal trajectory simulation. The setting of this coefficient was based on the debris drift simulation of the 2011 Japan tsunami (Maximenko et al., 2018). Additionally, Jones et al. (2016) reported that the horizontal movement of surface oil slicks is drifted by ~3.5% wind speed, including a 2% direct wind drag and a 1.5% wind speed adding to the surface Stokes drift (Abascal et al., 2009). The movements of free-floating

macroalgae are influenced by wind and windage, which depend on the physical characteristics of drifters. The hydrodynamic surface layer had already accounted for wind movement, and the other wind drag for particle drift was composed by direct windage. Based on the previous studies described above, the U. prolifera-induced total drifting windage was in a range of 2.7–3.5%. A series of particle tracking experiments were conducted in this windage range, with an interval of 0.1%. Meanwhile, one experiment without the direct wind factor was also undertaken for reference. Totally ten groups, with 1192 particles in every group, separated with a 0.02° horizontal resolution, were deployed in batches in the particle release zone (Fig. 3b) on May 1, 2014. These particles were traced for 120 days.

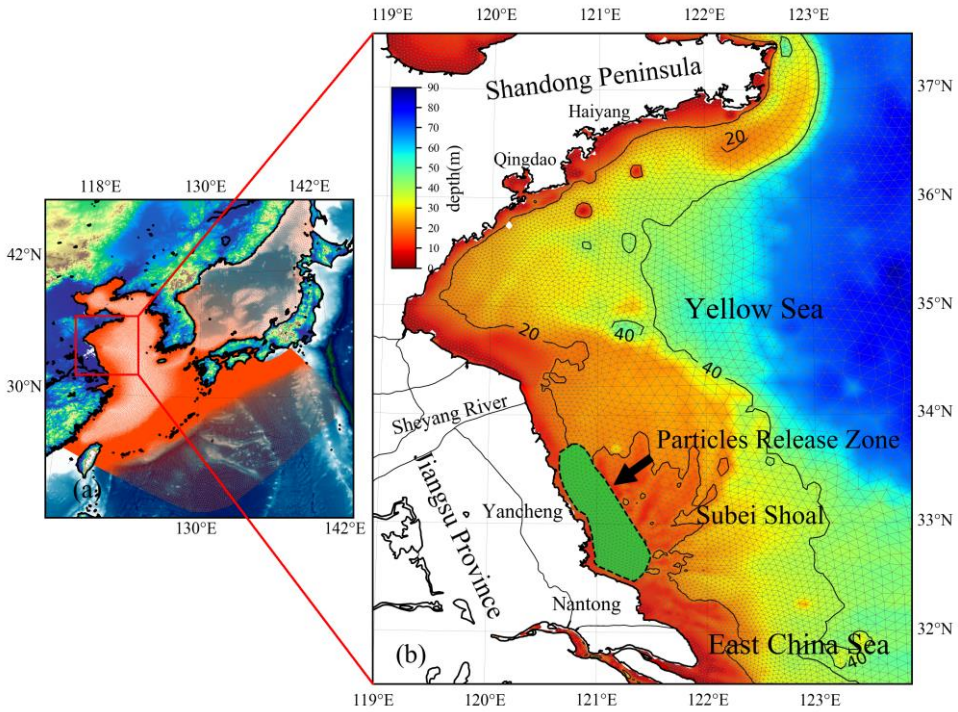

Figure 3(revised). (a) Location of YS, China. The red mesh indicates the high-resolution triangle grids of ECS-FVCOM. (b) The enlarged view of the area and bathymetry bounded by the solid red line rectangle in panel (a). The green area surrounded by a black dotted line in the Subei Shoal indicates the initial release zone of simulated particles.

Section *3.2:* "*Effects of physical factors"* in the original manuscript is changed to "*3.2 Tracking module evaluation*"

3.2.2 Windage simulation

The simulation results with different windages showed that particles first flowed northward and then turned northeastward (Fig. 9). With greater windage, the trend of northward transportation is more prominent. The particles with windage of about 3.4% could reach the southern coast of the Shandong Peninsula on June 15 (Fig. 9b) and then turned northeastward near 124°30.00'E (Fig. 9c–d). The particle group was split at the end of July. One part drifted northward continuously to 38°N and reached the North Korean coast, and the other was turned west (Fig. 9f). The particles with a windage coefficient less than 3.2 stranded near the southern coast of the Shandong Peninsula in July and August (Fig. 9d–f). The particles without direct windage have significantly slow drifting, northernmost nearly to the south coast of Shandong Peninsula. Some particles moved northeastward to the center of the South YS. From the comparison, winds contributed significantly to the transport of free-floating drifters. The transport results with a 2.7–3.5% windage range did not show a significant difference in the short-term simulation of 1–1.5 months (Fig. 9a–c). However, as the simulation time lasted longer, the transport pattern showed a noticeable difference (Fig. 9d–f). Compared with the evolution of green tides in the YS from remote sensing (Hu et al., 2019), it can be confirmed that the windage in a range of 3–3.2% could be applied to the drift of green tide. In this study, 3.2% was selected as the windage of the YS green tide simulation.

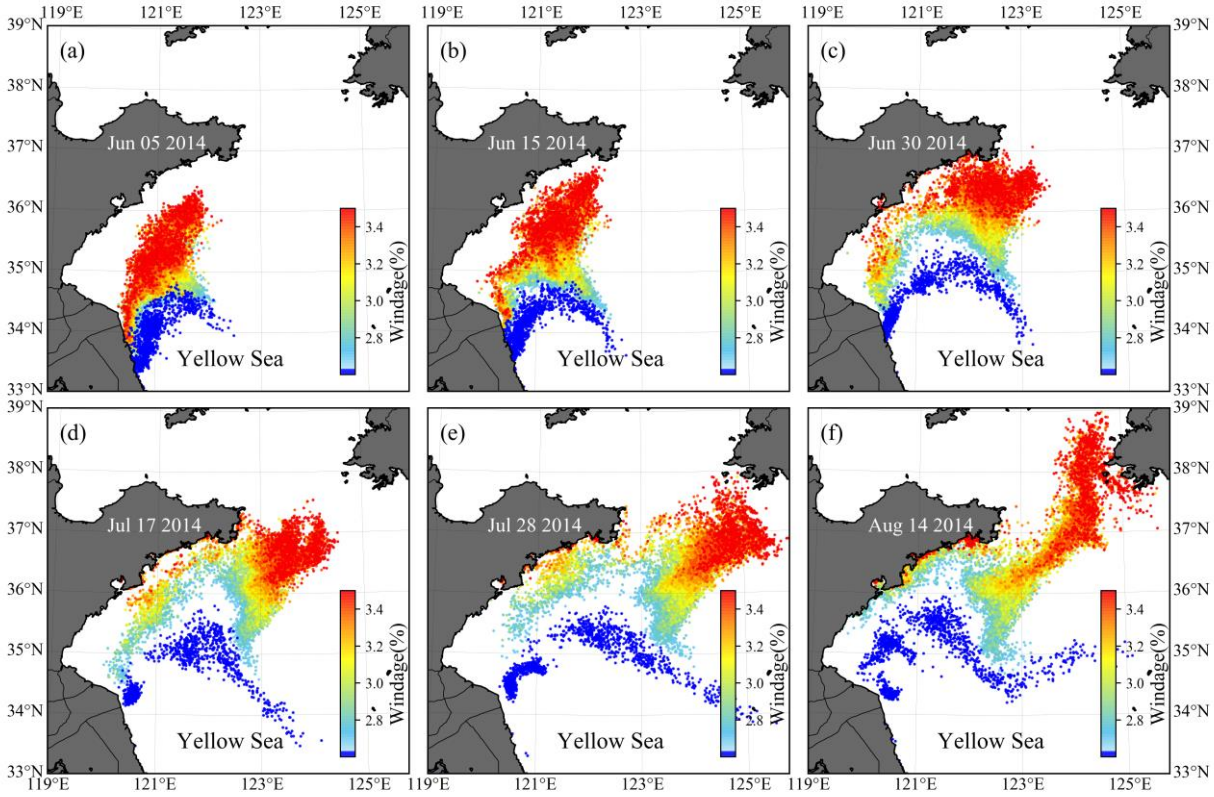

Figure. 9. Evolution of the particle distribution in FMGDM tracking simulations. Colors indicate different windage (2.7%-3.5%) of the simulated particles. The blue particles indicate the simulation without direct windage. (a) June 5, 2014; (b) June 15, 2014; (c) June 30, 2014; (d) July 17, 2014; (e) July 28, 2014; (f) August 14, 2014.

Reference:

Abascal, A. J., Castanedo, S., Mendez, F. J., Medina, R., and Losada, I. J.: Calibration of a Lagrangian Transport Model Using Drifting Buoys Deployed during the Prestige Oil Spill, Journal of Coastal Research, 25, 80-90, https://doi.org/10.2112/07-0849.1, 2009.

Chen, C., Zhao, L., Gallager, S., Ji, R., He, P., Davis, C., Beardsley, R. C., Hart, D., Gentleman, W. C., Wang, L., Li, S., Lin, H., Stokesbury, K., and Bethoney, D.: Impact of larval behaviors on dispersal and connectivity of sea scallop larvae over the northeast U.S. shelf, Progress in Oceanography, 195, 102604, https://doi.org/10.1016/j.pocean.2021.102604, 2021.

Dagestad, K.-F. and Röhrs, J.: Prediction of ocean surface trajectories using satellite derived vs. modeled ocean currents, Remote Sensing of Environment, 223, 130-142, https://doi.org/10.1016/j.rse.2019.01.001, 2019.

Hu, L., Zeng, K., Hu, C., and He, M.: On the remote estimation of Ulva prolifera areal coverage and biomass, Remote Sensing of Environment, 223, 194-207, https://doi.org/10.1016/j.ecss.2019.106329, 2019.

Maximenko, N., Hafner, J., Kamachi, M., and Macfadyen, A.: Numerical simulations of debris drift from the Great Japan Tsunami of 2011 and their verification with observational reports, Marine Pollution Bulletin, 132, 5-25, https://doi.org/10.1016/j.marpolbul.2018.03.056, 2018.

Whiting, J. M., Wang, T., Yang, Z., Huesemann, M. H., Wolfram, P. J., Mumford, T. F., and Righi, D.: Simulating the Trajectory and Biomass Growth of Free-Floating Macroalgal Cultivation Platforms along the U.S. West Coast, Journal of Marine Science and Engineering, 8, 938, https://doi.org/10.3390/jmse8110938, 2020.

The revision of tracking module evaluation:

2.5.3 Drifting trajectory data

The drifting dataset used to evaluate the skills of the tracking module is composed of two parts: the trajectory data of satellite-tracked surface drifters released from Subei Shoal in 2012 (Bao et al., 2015), and the subsurface drogued-float tracking data in the inner shelf of the East China Sea in 2017. All the original trajectory data are available at: https://doi.org/10.5281/zenodo.4616462.

3.2 Validation of Tracking module

3.2.1 Tracking module evolution

A total of seven satellite-tracked drogued-drifters were used to evaluate the skills of the particle tracking model, including five surface drifters released in the YS (Bao et al., 2015) and two subsurface drifters released in the ECS. The surface drifters contained four 40-cm width, 70-cm height rectangular sails, and a large central buoy (Bao et al., 2015). The subsurface drifter was constructed by a 67-cm diameter, 6-m height cylindrical subsurface sail, and a 28-cm diameter central buoy.

Seven particle-tracking simulations were conducted. One hundred particles were released at a location that matched the drifter's in-situ deployment position, and the horizontal random diffusion coefficient (K_r) was set as 50 m^2/s. In addition, the depth for surface and subsurface drifters were set as 0.5 m and 2 m, respectively. Thus, for these drogued-drifters, only half of the buoy was exposed above the sea surface, and the direct wind factor was not considered in the tacking simulations.

The simulated particle trajectories are generally consistent with the observed drifter trajectories, particularly for a short-term prediction (Fig. 8). The tracking time for surface drifters #1–5 lasted more than one month (Fig. 8a–e). The results show that the model was robust to reproduce the overall drifter's movement directions. Since the drifter paths may change with strong randomness due to complex variations of ocean flow, winds, and waves, the long-term prediction of drifter paths and dispersal could be of great challenge. The tracking time for subsurface drifters #6–7 (Fig. 8f) was relatively shorter, only 5–9 days. Compared with surface drifters, subsurface drifters were driven by a more complicated forcing relating to the large depth range of the sail. The water flow at a 2-m depth was selected as the driving force approximately, considering the average drifting state of subsurface drifters. The simulated trajectories were similar to the observed drifter's movement trends. However, the drifted distance was slightly shorter than the actual situation.

The model-data compression suggests that the particle tracking algorithm in FMGDM can provide reasonable predictions for free-floating drifters with higher confidence for surface drifters. In addition, the hydrodynamic model, ECS-FVCOM, is reliable. Our results showed that U. prolifera were mainly under a free-floating state at the sea surface.

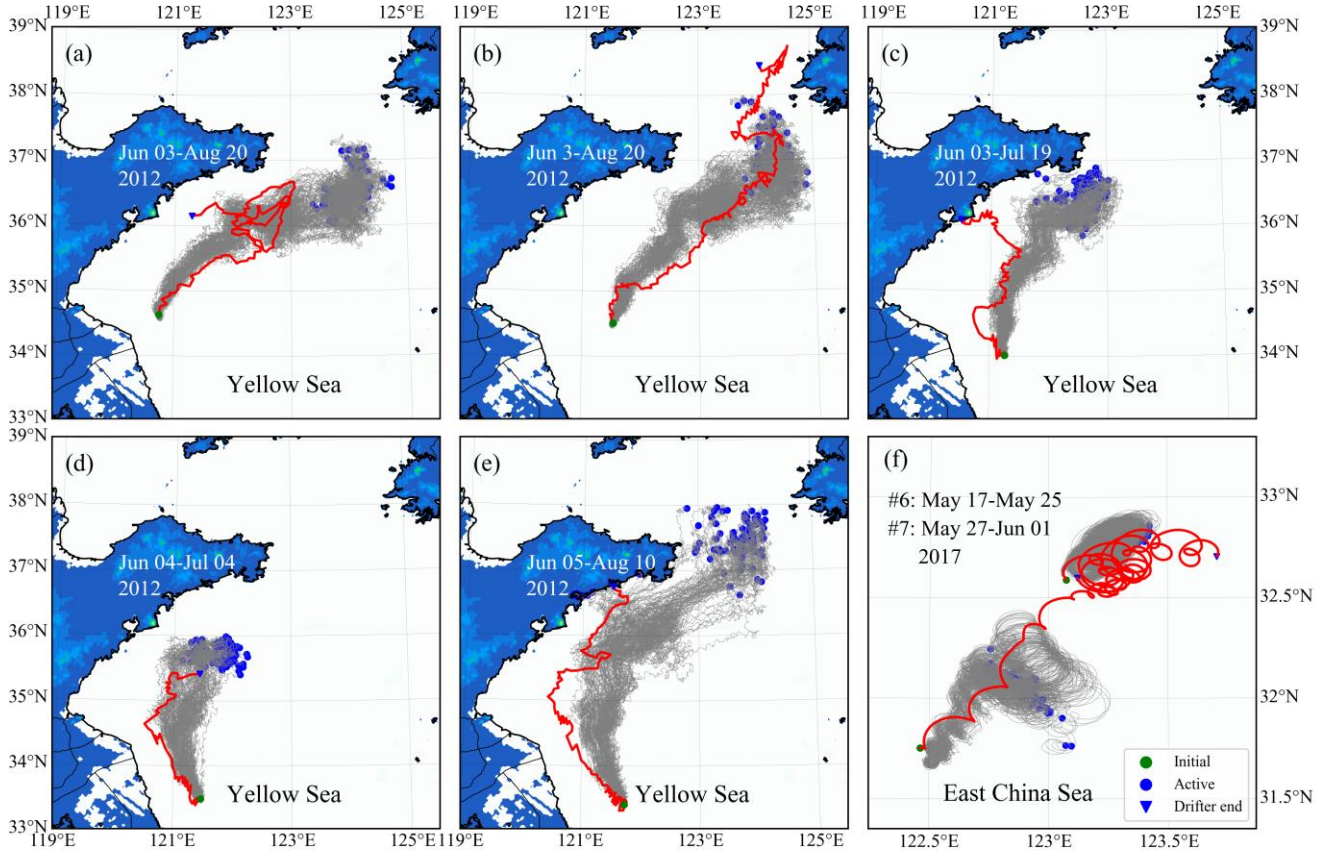

Figure. 8. Comparisons between observed (red lines) and simulated (grey lines) drifter trajectories.

Referee comment #2 and #3

From comment #2, part 2:

2. **The prolifera drifting experiment is carried out with an insufficient number of particles to capture the full ocean model variability, failing to convince the reader that the patterns obtained are robust. What's the rationale for deploying only 47 particles (each representing 100 tons of biomass), i.e. at 0.1° resolution on a single date (1st May), instead of for example deploying a particle in every gridcell of the model (resolution of 0.5 to 3km), together with a lower biomass per seeded particle, in that region, and repeated across the full period when U. prolifera is present in the area (mid-april to mid-May)? Are the results numerically stable with such low number?**

From comment #3, part 3:

3. **Model initialization is also important. The authors note a May 1 start time, several starting locations, and that 47 particles were used. More detail needs to be provided as to why the model was initialized this way. For example, 47 is far fewer particles than are typically used with trajectory modeling, so was computational cost the reason for so few particles?**

Response: Regarding the initial particle number (47), see our explanation above. We re-did the 2014 green tide simulation with ten times more particles at initial (480, each representing 10 tons of biomass). These particles were deployed evenly in the same release area (resolution of ~3 km) with settings as the same as those in the previous submission. It should be noted that the particle number increased during the growth process, reaching more than 1.8 million tons at the bloom peak (Fig. R1). It was nearly 400 times more than that at the initial state. Comparing with Fig. 9 in the last submission, there are no significant differences in the total biomass and the spatial patterns between the two simulation results.

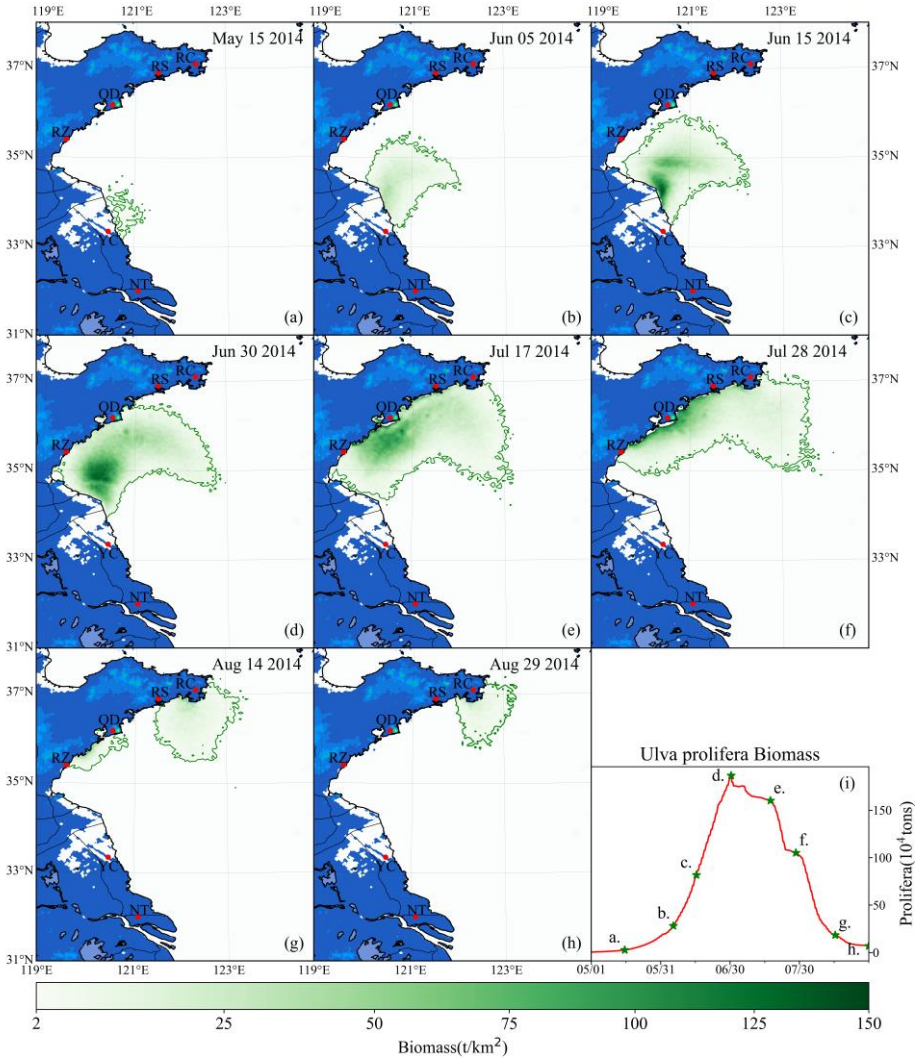

Figure R1 (for response). The 2014 green tide simulation, with 480 initial particles deployed with a separate scale of ~3 km.

We agree with the referees that adding simulated particles number is helpful to resolve the spatiotemporal flow variability. In subsequent simulations, the initially deployed particles were added by ten times, and each particle contained 10 tons of biomass. The selection of particles number was determined to have a balance between simulation accuracy and computational efficiency. More details could be found in the revision below. The settings of *U.prolifera* simulation were revised in section *2.7 model settings*

Most importantly, two realistic dynamic growth simulations were conducted. To verify the general applicability of the model, we simulated the growth and drift processes of U. prolifera in the YS in 2014 and 2015, respectively, with identical model configurations. In the two simulations, each particle represented 10 tone biomass of floating U. prolifera, so that 4,800 tons were deployed initially. The initial coverage and biomass of the U. prolifera were determined based on the field surveys by Liu et al. (2013) and Xu et al. (2014a). The simulation time was 135 days from April 16 to August 28. The initial particles deployed continuously from April 16 to May 15, 2014. Daily 160-ton biomass was spatial randomly released in the hot-spot zone (Fig. 3b) over an entire month. In this study, instantaneous environmental factors, including temperature, nutrients, solar radiation intensity, ocean flow, and wind speed, were determined from the physical ECS-FVCOM model.

Referee comment #2

3. **The ecological model could be better explained, in relation to the external factors chosen (and those disregarded) and enable the reader to get an understanding of how these factor influence growth/death. An equation of the prolifera dynamics over time as a function of these factors is needed. It seems though, that the model dynamics is simply driven by the laboratory-based measured rates for different ambient conditions, and that no physiological model exists. If this is not the case, it should be better explained, together with a sensitivity analsysis of the model parameters. Nutrients are known to influence macro algae growth, why is nutrient uptake not considered, using for example a biogeochemical model like in Brooks et al. (2018, Marine Ecology Progress). Only temperature causes mortality. What's the need for including salinity?**

We greatly appreciate this excellent suggestion. We have upgraded our ecological module in the revision by considering nutrient uptake in macroalgae growth. The literature provided by the referee, Brooks et al. (2018), developed an ecological model for *Sargassum*. Unfortunately, it is not applicable for the growth of *U.prolifera*. We found two studies in the ecological dynamic growth simulation of *Ulva* sp., which are more suitable for the ecological simulation of green tides (Ren et al., 2014; Sun et al., 2020). We adopted methodology from these studies to upgrade the ecological module in this revision. The physiological process was controlled by the function of temperature, irradiation, and nutrients. The original purpose of considering the salinity effect was to limit the growth of *U.prolifera* in low-salinity water., i.e., in the Changjiang River where the salinity was less than 25 PSU. However, this situation rarely occurred. The *U.prolifera* mainly grew in the high-salinity region. For this reason, the salinity limitation was removed from the biological module.

The revision of the section *2.1 Model framework*:

By contrast, in the macroalgae ecological module, the dynamic process of growth and mortality in the floating state are exhibited by particle replication and disappearance, and either the growth or mortality rate of each simulated particle is determined dynamically by the temperature, irradiation, and nutrients where the floating particle is in space and time. The position, velocity, quantity, and represented biomass of particles are updated synchronously between two modules. The physical and environmental factors are updated from the regional and local weather, ocean numerical model system, and marine atlas datasets. Based on the updated locations and biomasses of simulated particles, the coupled individual-based tracking and ecological model, applicable in the coverage and biomass simulation of floating macroalgae, is achieved.

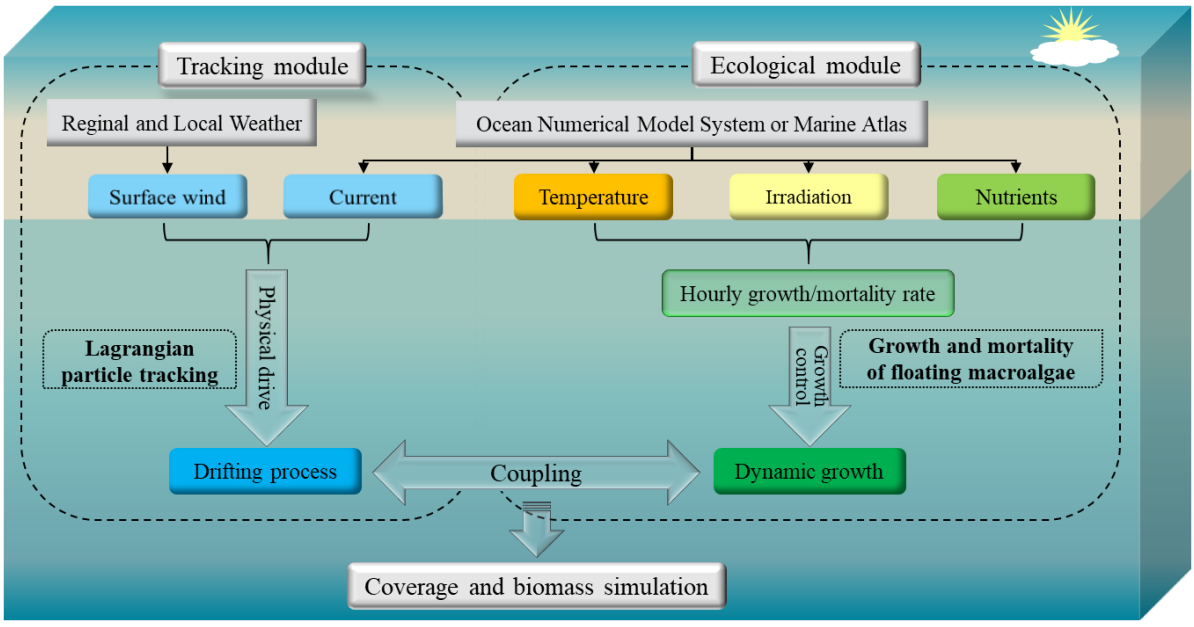

Figure 1(revised). Framework of the physical–ecological coupled model FMGDM v1.0.

The revision of the section *2.3 Ecological module*:

2.3 Ecological module

The ecological module reflects the growth and extinction of macroalgae by the replication and extinction of particles. One initial particle represented a patch with fixed biomass (m_0) of floating macroalgae, and the value could be adjusted according to needs. It was replicated and randomly released within a 2-km radius of the original location when the represented biomass of the particle exceeded $2m_0$. The biomass of the two particles returned to the initial value m_0. Both particles then undergo drifting and growth/extinction processes independently (Fig. 2a). Additionally, when two nearby particles had biomass below $0.5m_0$, they were combined to form one particle with m_0, representing the extinction process (Fig. 2b).

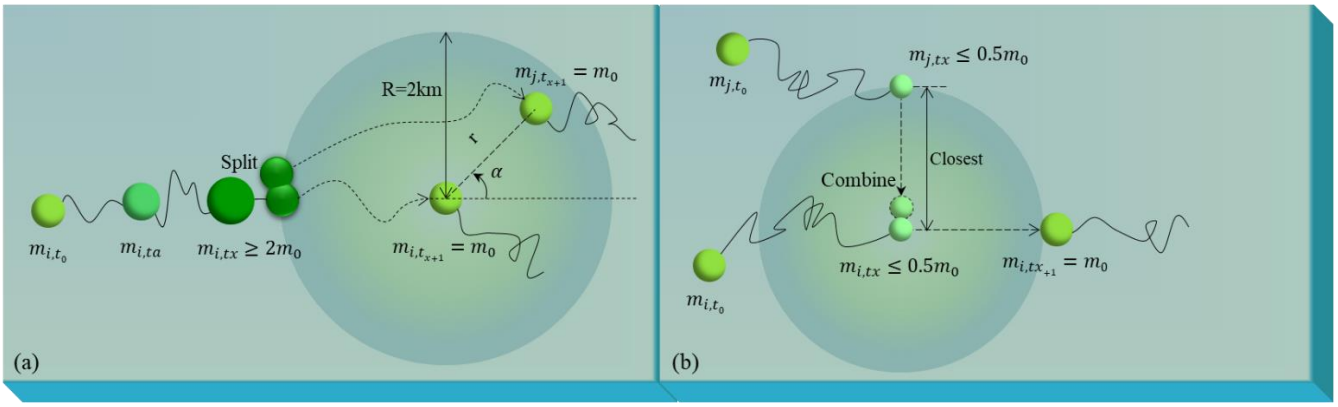

Figure 2. Diagram of the replication (a) and extinction (b) process of simulated macroalgae represented by particles.

The macroalgae growth structure of this ecological module refers to the Ulva sp. growth models established by Ren et al. (2014) and Sun et al. (2020). The physiological process of this module is reflected in the absorption and loss of carbon (C), nitrogen (N), and phosphorus (P). Their uptake rates were represented as V_c, V_N, and V_P, respectively. The loss rates were represented as L_c, L_N, and L_P, respectively. The calculation of dynamic change of single-particle was expressed as:

$$\frac{dC}{dt} = V_c - L_c \quad (5)$$

$$\frac{dN}{dt} = V_N - L_N \quad (6)$$

$$\frac{dP}{dt} = V_P - L_P \quad (7)$$

We expressed the biomass evolution as carbon. The fresh weight (FW) could be determined by

$$FW = \frac{C}{K_{TOC}} \quad (8)$$

where K_{TOC} indicates the conversion ratio between C and FW. Based on the physiological characteristics, the conversion value between C and FW was set as 8 mmol C /gFW (Sun et al., 2020).

The total biomass (M_t) of floating macroalgae throughout the domain can be determined by summing up the biomass of all active particles.

$$M_t = \sum_{n=1}^{N_t} FW_{t,n} \quad (9)$$

The uptake and loss of C, N, and P are controlled by the photosynthesis, respiration, and mortality processes, proportional to biomass. The absorption of C is dependent on the function of photosynthesis $f(I)$, limited by the functions of temperature $f_p(T)$, nutrients $f(N)$, and light attenuation of self-shading by macroalgae $f(\rho)$.

$$V_c = f(I)f_p(T)f(N)f(\rho)\cdot C \quad (10)$$

where $f(\rho)$ is the effect of self-shading depends on the type of macroalgae and assembled density ρ (mol C/m^2). The photosynthesis function $f(I)$ indicates the relation between photosynthesis and irradiation I (Jassby and Platt, 1976).

$$f(I) = P_{max}tanh\left(\frac{\alpha I}{P_{max}}\right) \quad (11)$$

where P_{max} is the maximum photosynthetic rate and α is the photosynthetic efficiency. The changes in internal nutrients quotas have a significant impact on the physiological processes of macroalgae. The N-quota (Q_N) and the P-quota (Q_P) represented N:C and P:C, respectively (Ren et al., 2014). The relationship between nutrient quotas and photosynthesis is referred to Droop (1968). Q_{Nmin} and Q_{Pmin} are the minimum quota of N and P, respectively.

$$f(N) = min\left[\frac{Q_N - Q_{Nmin}}{Q_N}, \frac{Q_P - Q_{Pmin}}{Q_P}\right] \quad (12)$$

The nutrient uptake rate is controlled by the concentration of N and P, and limited by the functions of temperature $f_p(T)$ and absorption attenuation caused by macroalgae accumulation $f(\rho)$. The functions of nutrients uptake rate are referred to Lehman et al. (1975). The absorption of nutrients by macroalgae mainly considers dissolved inorganic nitrogen (DIN) and dissolved inorganic phosphate (DIP). The uptake rate of DIN and DIP are represented as V_{DIN} and V_{DIP}, respectively. They are calculated as

$$V_{DIN} = V_{mDIN}\frac{C_{DIN}}{K_{DIN} + C_{DIN}}\frac{Q_{Nmax} - Q_N}{Q_{Nmax} + Q_{Nmin}}\cdot f_P(T)f(\rho)\cdot C \quad (13)$$

$$V_{DIP} = V_{mDIP}\frac{C_{DIP}}{K_{DIP} + C_{DIP}}\frac{Q_{Pmax} - Q_P}{Q_{Pmax} + Q_{Pmin}}\cdot f_P(T)f(\rho)\cdot C \quad (14)$$

The maximum uptake rate of DIN and DIP are represented as V_{mDIN} and V_{mDIP}, respectively. The concentration of DIN and DIP are expressed as C_{DIN} and C_{DIP}, respectively. The half-saturation coefficient for DIN and DIP are represented as K_{DIN} and K_{DIP}, respectively (Sun et al., 2020). Q_{Nmax} and Q_{Pmax} are the maximum quota of N and P, respectively.

The C loss is contributed by respiration and mortality. The C loss of respiration depends on the temperature-related function $f_r(T)$. The C loss of mortality depends on irradiance-related function $f(I)$, nutrients-related function $f(N)$ and temperature-related function $f_m(T)$. The temperature limitation functions, $f_p(T)$, $f_r(T)$, and $f_m(T)$, corresponds to photosynthesis, respiration, and mortality processes, respectively, where R_d is the dark respiration rate. When the temperature is unsuitable for the survival of macroalgae, $f_r(T)$ keeps to a minimum value indicating that minimal respiration. The mortality process replaces photosynthesis as the dominant under severe temperature and light intensity.

Similar to the loss of C, the uptake and loss of N and P are controlled by the respiration processes, and they are also proportional to biomass. The loss rate of C, N, and P can be calculated by

$$L_c = R_d f_r(T)\cdot C + f(I)f_m(T)f(N)\cdot C \quad (15)$$

$$L_{DIN} = R_d Q_N f_d(T)\cdot C \quad (16)$$

$$L_{DIP} = R_d Q_P f_d(T)\cdot C \quad (17)$$

It should be noted that there is no interaction between this ecological module and the ocean numerical model system since this model is designed for offline computation, which is driven by the ocean model output of physical and ecosystem simulation.

2.7 Model settings

We set the parameters of the ecological module according to the physiological characteristics of U. prolifera. The functions of temperature were determined referring to the results of laboratory studies. U. prolifera has the optimal photosynthesis efficiency at 20 °C, and turns white and declines rapidly under high temperature and high light intensity (Cui et al., 2015; Song et al., 2015). When the temperature is suitable (5–25.7 °C), the temperature limitation of photosynthesis $f_p(T)$ and respiration $f_r(T)$ are consistent. When the temperature becomes unsuitable (<5 °C or >25.7 °C), the respiration of macroalgae, unlike photosynthesis, will remain at a lower level. When the high temperature exceeds a suitable situation (>25.7 °C), the mortality process replaced photosynthesis as dominance.

$$f_p(T) = \begin{cases} -4.942 \times 10^{-4}T^3 + 0.01885T^2 - 0.135T + 0.1014, 5°C \le T \le 25.7°C \\ 0, T < 5°C \ or \ 25.7°C < T \end{cases} \quad (18)$$

$$f_r(T) = \begin{cases} -4.942 \times 10^{-4}T^3 + 0.01885T^2 - 0.135T + 0.1014, 5°C \le T \le 25.7°C \\ 0.789, T < 5°C \ or \ 25.7°C < T \end{cases} \quad (19)$$

$$f_m(T) = \begin{cases} 0, T \le 25.7°C \\ 0.01416T^3 - 1.223T^2 + 35.22T - 337.73, T \ge 25.7°C \end{cases} \quad (20)$$

According to the floating growth characteristics of U. prolifera, the self-shading limited function $f(\rho)$ was determined. When the assembled density does not exceed 0.16 mol C/m^2, the growth of U. prolifera is not restricted by self-shading. However, as the density increases, the accumulation of U. prolifera becomes significant, and maximum when the density is greater than 0.56 mol C/m^2.

$$f(\rho) = \begin{cases} 1, \rho \le 0.16 \\ 2.308\, exp(-2.5\rho) - 0.54705, 0.16 < \rho \le 0.56 \\ 0, \rho > 0.56 \end{cases} \quad (21)$$

The complete list of parameters used in the ecological module of U. prolifera was shown in Table. 1.

Table. 1. Parameters used in ecological module for U.prolifera, modified from Sun et al. (2020).

Parameters	Description	Value	Dimension	Reference
Q_{Nmin}	Minimum N-quota	25.3	$mmol\ N\ mol\ C^{-1}$	(Fujita, 1985)
Q_{Nmax}	Maximum N-quota	108.7	$mmol\ N\ mol\ C^{-1}$	(Sun et al., 2015)
Q_{Pmin}	Minimum P-quota	0.097	$mmol\ N\ mol\ C^{-1}$	(Sfriso et al., 1990)
Q_{Pmax}	Maximum P-quota	1.4	$mmol\ N\ mol\ C^{-1}$	(Sun et al., 2015)
V_{mDIN}	Maximum uptake rate of DIN	2.8	$mmol\ N\ mol\ C^{-1}h^{-1}$	(Li and Zhao, 2011; Luo et al., 2012)
V_{mDIp}	Maximum uptake rate of DIP	0.58	$mmol\ N\ mol\ C^{-1}h^{-1}$	(Luo et al., 2012)
K_{DIN}	Half-saturation coefficient for DIN	18.77	$\mu mol\ N\ L^{-1}$	(Li and Zhao, 2011; Luo et al., 2012)
K_{DIP}	Half-saturation coefficient for DIP	10	$\mu mol\ N\ L^{-1}$	(Luo et al., 2012)
P_{max}	Maximum photosynthetic rate	240.51	$\mu mol\ C\ g\ WW^{-1}h^{-1}$	(Xu et al., 2014b)
α	Photosynthetic efficiency	2.52	$(\mu mol\ C\ g\ WW^{-1}h^{-1})$ $/(\mu mol\ photons\ m^{-2}s^{-1})$	(Xu et al., 2014b)
R_d	Dark respiration rate	18.4	$\mu mol\ C\ g\ WW^{-1}h^{-1}$	(Xu et al., 2014b)

The revision of the section *2.5 Data sources*:

2.5.3 Nutrients data

The seasonal nitrate and phosphate datasets of YS are obtained from the World Ocean Atlas 2018 (Garcia H.E. et al., 2019), with a spatial resolution of 1 degree, and merged with the datasets from the marine atlas of the Yellow Sea (Wang et al., 1991). With combined two datasets, the nutrients at the sea surface (April to August) are applied to this simulation through temporal interpolation.

The revision of the section *3.1 Variations of environmental factors:*

3.1.5 Dissolved nutrients

The dissolved inorganic nutrients in the offshore region are mainly influenced by terrestrial sources, with prominent seasonal characteristics. The concentration of dissolved inorganic nutrients in the Jiangsu region was significantly higher than in other areas. The nitrate concentration in the offshore region of Jiangsu was generally above 2 mmol/m^3 in spring (Fig. 7a) and summer (Fig. 7b), especially in the Yancheng region, the nitrate concentration was over 8 mmol/m^3 in spring (Fig. 7a). The nitrate concentration in the other areas of YS, except the offshore region of Jiangsu, was mainly below 2 mmol/m^3. The phosphate concentration in the offshore region of Nantong and Sheyang River Estuary was still high, more than 0.6 mmol/m^3 in spring (Fig. 7c) and summer (Fig. 7d). In the north of Yancheng offshore region, phosphate concentration decreased to ~0.2 mmol/m^3 in summer (Fig. 7d). In the central YS and south offshore area of Shandong Peninsula, phosphate concentration was higher in summer, over 0.2 mmol/m^3, than ~0.1 mmol/m^3 in spring.

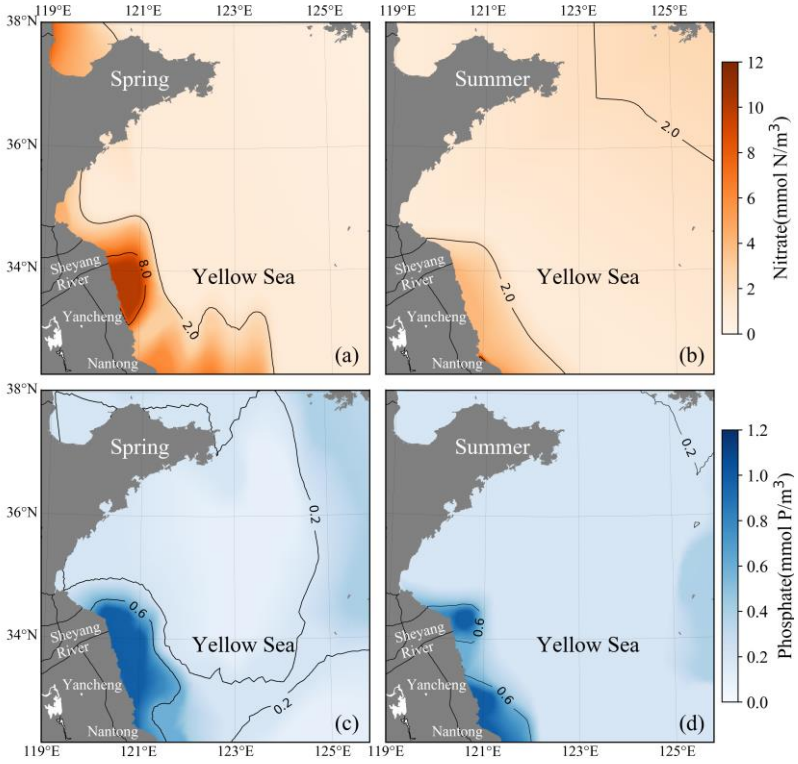

Figure. 7. Seasonal-averaged surface distributions of nitrate (upper) and phosphate (lower) in YS during spring (left), summer (right).

The revision of the section *3.3.1 Spatiotemporal variation of U. prolifera*:

3.3.1 Spatiotemporal variation of U. prolifera

After being released into Subei Shoal, the initial particles drifted and dispersed by ocean flows and wind. The simulation result of the green tide in 2014 is shown in Fig. 10. It showed a small amount of U. prolifera floating on the Subei coast in mid-May (Fig.10a). However, it was difficult to be observed using remote sensing technology in the early stage of green tide bloom. After one month of simulation, the modeling biomass increased to approximately 0.2 million tons (Fig. 10i) on June 5. Both the results of observation and simulation showed that U. prolifera was transported northward and floated between northern Jiangsu offshore and Shandong Peninsula (Fig. 10b). On June 15 (Fig. 10c), observation shows that green tides had landed on the southern coast of Shandong Peninsula, including Rizhao (RZ) and Qingdao shore. Meanwhile, the floating simulation was also close to these two sites. Moreover, observation shows that green tides bloomed around the coast of Nantong (NT) and Yancheng (YC), suggesting the continuous release of additional U. prolifera from aquaculture raft between May and June 2014. On June 23 (Fig. 10d), the result of both observation and simulation were consistent and showed that green tides had landed on the Shandong Peninsula on a large scale, and the farthest U. prolifera reached the Rushan (RS) coast. The entire coastal and offshore regions were covered with a huge amount of floating U. prolifera. Due to the high concentration of nutrients, there were a large number of simulated particles growing at the Sheyang River estuary region in the entire June. The biomass of simulation reached a peak of 0.98 million tons on June 30 (Fig. 10i). Subsequently, U. prolifera died out quickly, and its coverage decreased significantly. On July 17 (Fig. 10f), the floating U. prolifera still gathered on the south coast of the Shandong Peninsula. In contrast with the simulation results, observation showed the re-occurrence of a large-scale green tide in Yancheng and Nantong regions, which, however, was uncaptured by the model. Both observation and simulation results show that floating U. prolifera drifted eastward but still covered the south coast of the Shandong Peninsula at the end of July (Fig. 10g). After half a month, floating U. prolifera had died out (Fig. 10h). Observation shows that only the southern coast of Qingdao and Subei Shoal had a few patches of U. prolifera on August 14, which suggests there is still a possible U. prolifera source near Subei Shoal even in the summertime of July and August. However, the U. prolifera of simulation had almost vanished because the U. prolifera source was only initialized from mid-April to mid-May.

As there was no direct way of quantifying the floating U. prolifera biomass of green tides throughout the YS (Wang et al., 2018), the estimated biomass data of U. prolifera retrieved from remote sensing observations (Hu et al., 2019) was adopted to validate the simulated biomass (Fig. 10i). The estimated biomass of U. prolifera rose rapidly and peaked with maximum values of 0.92 million tons on June 18, 2014. The biomass declined rapidly after reaching its peak, and U. prolifera almost died off at the end of July. Compared with observation results, the biomass of simulation peaked after 12 days with a similar value. The growth trends between observation and simulation were similar. Considering the highly random dispersion, as well as the dynamic life history of U. prolifera, our simulation provides reasonable modeling results of biomass and spatial coverage.

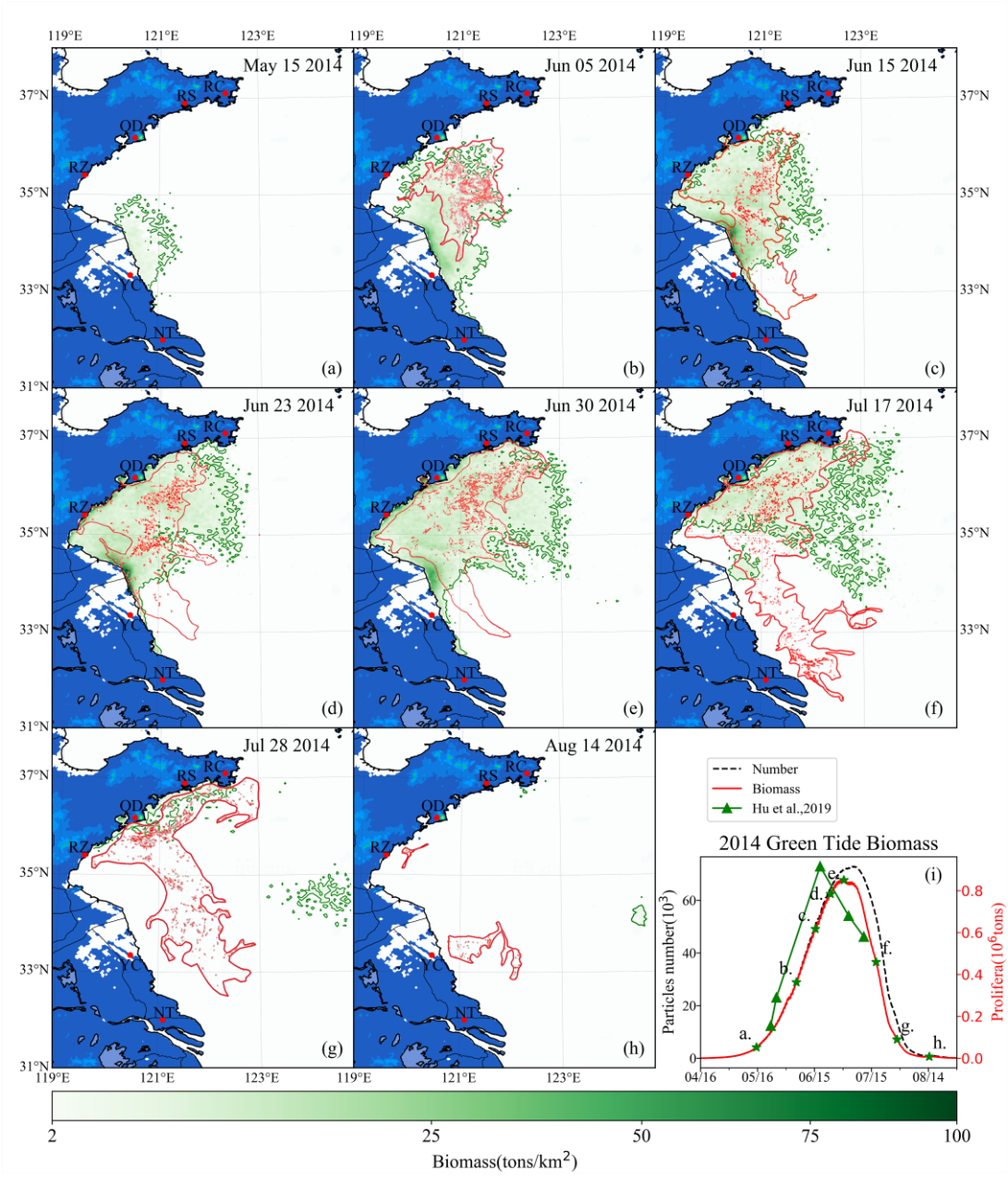

Figure 10(revised). Comparison between simulation and remote sensing observation of green tides from May to August 2014 (a–h). The green image indicates the simulated biomass density of green tides (color image, unit: tons/km^2). The red image shows the satellite-derived spatial coverage of U. prolifera from MODIS-TERRA. Panel (i) is the time series of simulated biomass and particle number of green tides in 2014, compared with observed biomass from Hu et al. (2019). The green pentagram in panel (i) indicates the biomass of the corresponding date in the panel (a–h).

Referee comment #2

4. **The model reproduces the bloom dynamics to first order, yet little year to year variability is present in the spatial patterns for the two years of the study, although a clear inter-annual signal exists in the observations. For instance large parts of prolifera patches in July 2018 are uncaptured by the model. It is not possible to determine what is the cause for these dicrepancies (biological or physical?). I wonder whether a better choice of particle deployment at start (as mentioned above) would improve the results. In support, we see that short term simulation (1 week) show better skills. Could this be explained by a better initialisation? An analysis (or inverse modelling approach)**

would be useful to get a feeling of the sensitivity to the choice of parameter values (whether physical or ecological) for best recreating the observed biomass concentrations.

In this study, we only simulated the bloom of YS green tides from spring to summer, assuming all green algae die in late summer. However, according to the related studies (Liu et al., 2012; Zhang et al., 2009), limited green algae could overwinter and restore growth in next spring in offshore and central YS. Therefore, the correlation between two consecutive years was limited but still exists. Meanwhile, the annual variability in the bloom biomass and spatial patterns significantly correlates with the initial biomass and origin place in different years. Limited by the difficulty of comprehensive in-situ investigation and consequently lack information for biomass and coverage, we had to make the simulation for 2014 and 2015 with the same initialization of biomass and spatial patterns. We determined the initial biomass of about 5,000 tons by Liu et al. (2013) and Xu et al. (2014a) and deployed in the coast of Yancheng and Nantong, the main origin areas of *U. prolifera*.

About the large parts of *U.prolifera* patches uncaptured by the model, it should be the results in July 2014. We had discussed that in the section as follows:

4.3 Roles of initial biomass and nutrient limitation

The existence of diverse origins and continuous input of floating propagules significantly challenge the precise prediction and effective control of massive floating macroalgal blooms. In addition to the extensive provision from Porphyra aquaculture rafts in the Subei Shoal, the somatic cells, indicated by a laboratory study, could overwinter and restore growth on the annual spring bloom (Zhang et al., 2009), which is another significant source of U. prolifera. Additionally, four overwintering Ulva propagules that existed in sediments, including U. prolifera, may recover their growth when the temperature and irradiation are appropriate (Liu et al., 2012). Every April, before the occurrence of green tides, Ulva propagules are already widespread on the southern coast of the YS (Yuanzi et al., 2014). The transport trajectory was strongly affected by the origin of U. prolifera. Under the same environmental conditions, the scale of the bloom was determined primarily by the initial organisms. During the macroalgal bloom, the propagules supply from the coastal waters is continuously uncertain and difficult to determine through satellite observations or in situ surveys. Therefore, the feature that there was still large-scale U. prolifera distribution around the Subei Shoal in June and July 2014 has not yet been captured, as shown by satellite observations (Fig. 10), despite the continuous entering during the period of Porphyra aquaculture rafts collection (mid-April to mid-May) has been considered in the green tide simulations.

As the referee mentioned, a better choice of particle deployment as initialization would improve the results. Remote sensing observation was the most effective way to get the spatial patterns of the green tide. The short-term simulation showed better skills when the model was initialized with the spatial distribution of green tide by remote sensing data.

The inverse tracking could provide a reasonable estimation of position for a short time. However, with 1–2 month inverse tracking, the model still fails to estimate the origin place of the green tide, covering a significantly large area. This overestimation of origin place is more significant when considering the random walk process in the tracking algorithm. We have tried to deployed initial particles continuously across an entire month (mid-April to mid-May). However, the *U.prolifera* floating in the Jiangsu region in July was still difficult to reproduce, which suggests there is still a possible *U. prolifera* source near Subei Shoal even in the summertime of July and August.

Referee comment #3

2. **Most trajectory models also include dispersion to represent forcings not caused by wind or currents. This dispersion is often a stochastic component. If the authors determine not to include dispersion in their model simulations, there should at least be acknowlegement of the absence of dispersion and resulting implications.**

The random dispersion had already been included in the model, which was considered as horizontal and vertical random walk by adding extra terms to particle trajectory calculation. Since the *U. prolifera* mainly floats at the sea surface without the vertical migration, the vertical random walk was disabled in the model setting. We have clarified that in the revision to better highlight the model capability and configuration on random dispersion as follows:

Dispersion, which was not caused by wind or currents, is also included in the trajectory tracking module. It mainly exhibited a stochastic movement, which was considered horizontal and vertical random walks by adding extra terms to particle trajectory calculation. Since the macroalgae mainly float at the sea surface without significant vertical migration, the vertical random walk was not turned on in the model setting. The horizontal random diffusion of the particles $\Delta\overrightarrow{x_r}$ *is considered in simulation as Eq. 3. The coefficient of horizontal random diffusion,* K_r *(unit: m²/s), and the time step for random diffusion was set to 6 s according to Visser's criterion. The unit vector* $\vec{a}$ *takes a random direction angle, and the random number* R*, fits normal distribution, takes a value between 0 and 1.0.*

$$\Delta\overrightarrow{x_r}(\Delta t) = \vec{a} \cdot R\sqrt{2K_r\Delta t} \qquad (3)$$

Therefore, the final position of Lagrangian particle-tracking during one-time step Δt *can be expressed as:*

$$X_{t+\Delta t} = X_t + \int_t^{t+\Delta t} \vec{V}(x_t, t)dt + \Delta\overrightarrow{x_r}(t) \qquad (4)$$

The value of K_r was set in the section *2.7 Model settings*:

The horizontal random diffusion K_r *of the green tide simulation was set as 200 m²/s.*

Reference:

Bao, M., Guan, W., Yang, Y., Cao, Z., and Chen, Q.: Drifting trajectories of green algae in the western Yellow Sea during the spring and summer of 2012, Estuarine, Coastal and Shelf Science, 163, 9-16, https://doi.org/10.1016/j.ecss.2015.02.009, 2015.

Cui, J., Zhang, J., Huo, Y., Zhou, L., Wu, Q., Chen, L., Yu, K., and He, P.: Adaptability of free-floating green tide algae in the Yellow Sea to variable temperature and light intensity, Marine Pollution Bulletin, 101, 660-666, https://doi.org/10.1016/j.marpolbul.2015.10.033, 2015.

Droop, M. R.: Vitamin B12 and Marine Ecology. IV. The Kinetics of Uptake, Growth and Inhibition in Monochrysis Lutheri, Journal of the Marine Biological Association of the United Kingdom, 48, 689-733, https://doi.org/10.1017/s0025315400019238, 1968.

Fujita, R. M.: The role of nitrogen status in regulating transient ammonium uptake and nitrogen storage by macroalgae, Journal of Experimental Marine Biology and Ecology, 92, 283-301, https://doi.org/10.1016/0022-0981(85)90100-5, 1985.

Garcia H.E., K.W. Weathers, C.R. Paver, I. Smolyar, T.P. Boyer, R.A. Locarnini, M.M. Zweng, A.V. Mishonov, O.K. Baranova, D. Seidov, and Reagan, a. J. R.: World Ocean Atlas 2018. Vol. 4: Dissolved Inorganic Nutrients (phosphate, nitrate and nitrate+nitrite, silicate, NOAA Atlas NESDIS 84, 35pp, https://archimer.ifremer.fr/doc/00651/76336/, 2019.

Hu, L., Zeng, K., Hu, C., and He, M.: On the remote estimation of Ulva prolifera areal coverage and biomass, Remote Sensing of Environment, 223, 194-207, https://doi.org/10.1016/j.ecss.2019.106329, 2019.

Jassby, A. D. and Platt, T.: Mathematical formulation of the relationship between photosynthesis and light for phytoplankton, Limnology and Oceanography, 21, 540-547, https://doi.org/10.4319/lo.1976.21.4.0540, 1976.

Lehman, J. T., Botkin, D. B., and Likens, G. E.: The assumptions and rationales of a computer model of phytoplankton population dynamics1, Limnology and Oceanography, 20, 343-364, https://doi.org/10.4319/lo.1975.20.3.0343, 1975.

Li, J. and Zhao, W.: Effects of nitrogen specification and culture method on growth of Enteromorpha prolifera, Chinese Journal of Oceanology and Limnology, 29, 874-882, https://doi.org/10.1007/s00343-011-0516-6, 2011.

Liu, D., Keesing, J. K., He, P., Wang, Z., Shi, Y., and Wang, Y.: The world's largest macroalgal bloom in the Yellow Sea, China: Formation and implications, Estuarine, Coastal and Shelf Science, 129, 2-10, https://doi.org/10.1016/j.ecss.2013.05.021, 2013.

Liu, F., Pang, S. J., Zhao, X. B., and Hu, C. M.: Quantitative, molecular and growth analyses of Ulva microscopic propagules in the coastal sediment of Jiangsu province where green tides initially occurred, Marine Environmental Research, 74, 56-63, https://doi.org/10.1016/j.marenvres.2011.12.004, 2012.

Luo, M. B., Liu, F., and Xu, Z. L.: Growth and nutrient uptake capacity of two co-occurring species, Ulva prolifera and Ulva linza, Aquatic Botany, 100, 18-24, https://doi.org/10.1016/j.aquabot.2012.03.006, 2012.

Ren, J. S., Barr, N. G., Scheuer, K., Schiel, D. R., and Zeldis, J.: A dynamic growth model of macroalgae: Application in an estuary recovering from treated wastewater and earthquake-driven eutrophication, Estuarine, Coastal and Shelf Science, 148, 59-69, https://doi.org/10.1016/j.ecss.2014.06.014, 2014.

Sfriso, A., Marcomini, A., Pavoni, B., and Orio, A. A.: Eutrofizzazione e macroalghe: la Laguna di Venezia come caso esemplare, Inquinamento, 4, 62-78, 1990.

Song, W., Peng, K., Xiao, J., Li, Y., Wang, Z., Liu, X., Fu, M., Fan, S., Zhu, M., and Li, R.: Effects of temperature on the germination of green algae micro-propagules in coastal waters of the Subei Shoal, China, Estuarine, Coastal and Shelf Science, 163, 63-68, https://doi.org/10.1016/j.ecss.2014.08.007, 2015.

Sun, K.-M., Li, R., Li, Y., Xin, M., Xiao, J., Wang, Z., Tang, X., and Pang, M.: Responses of Ulva prolifera to short-term nutrient enrichment under light and dark conditions, Estuarine, Coastal and Shelf Science, 163, 56-62, https://doi.org/10.1016/j.ecss.2015.03.018, 2015.

Sun, K., Ren, J. S., Bai, T., Zhang, J., Liu, Q., Wu, W., Zhao, Y., and Liu, Y.: A dynamic growth model of Ulva prolifera: Application in quantifying the biomass of green tides in the Yellow Sea, China, Ecological Modelling, 428, 109072, https://doi.org/10.1016/j.ecolmodel.2020.109072, 2020.

Wang, Y., Lu, S., Huang, S., Wang, Z., Liu, J., Wu, C., Wu, H., Chen, Y., Li, P., Zhang, S., Zhang, Z., Zhao, D., Tang, R., Jiang, G., and Tan, M.: Marine Atlas of Bohai Sea, Yellow Sea, East China Sea: Chemistry, China Ocean Press, 1991.

Wang, Z., Fu, M., Xiao, J., Zhang, X., and Song, W.: Progress on the study of the Yellow Sea green tides caused by Ulva prolifera., Acta Oceanologica Sinica, 40, 1-13, https://doi.org/10.3969/j.issn.0253-4193.2018.02.001, 2018.

Xu, Q., Zhang, H., Ju, L., and Chen, M.: Interannual variability of Ulva prolifera blooms in the Yellow Sea, International Journal of Remote Sensing, 35, 4099-4113, https://doi.org/10.1080/01431161.2014.916052, 2014a.

Xu, Z., Wu, H., Zhan, D., Sun, F., Sun, J., and Wang, G.: Combined effects of light intensity and NH 4 + -enrichment on growth, pigmentation, and photosynthetic performance of Ulva prolifera (Chlorophyta), Chinese Journal of Oceanology and Limnology, 32, 1016-1023, https://doi.org/10.1007/s00343-014-3332-y, 2014b.

Yuanzi, H., Liang, H., Hailong, W., Jianheng, Z., Jianjun, C., Xiwen, H., Kefeng, Y., Honghua, S., Peimin, H., and Dewen, D.: Abundance and distribution of Ulva microscopic propagules associated with a green tide in the southern coast of the Yellow Sea, Harmful Algae, 39, 357-364, https://doi.org/10.1016/j.hal.2014.09.008, 2014.

Zhang, X., Wang, H., Mao, Y., Liang, C., Zhuang, Z., Wang, Q., and Ye, N.: Somatic cells serve as a potential propagule bank of Enteromorpha prolifera forming a green tide in the Yellow Sea, China, Journal of Applied Phycology, 22, 173-180, https://doi.org/10.1007/s10811-009-9437-6, 2009.